Role of lactam *vs*. lactim tautomers in 2(1*H*)-pyridone catalysis of aromatic nucleophilic substitution

Anne Loppinet-Serani, Florence Charbonnier,* Christian Rolando † and Ivan Huc ‡

Ecole Normale Supérieure, Département de Chimie, URA 1679 du CNRS, Processus d'Activation Moléculaire, 24 rue Lhomond, 75231 Paris Cedex 05, France

3-Ethylaminocarbonyl-2(1*H*)-pyridone 1 and 3-ethoxycarbonyl-2(1*H*)-pyridone 2 have been synthesised and tested as catalysts for the aromatic nucleophilic substitution of fluoride by piperidine in 2-fluoro-5-nitrobenzonitrile 3. A kinetic model which takes into account the dimerisation of the catalysts has been developed, which allows a quantitative analysis of measured data. 3-Ethylaminocarbonyl-2(1*H*)-pyridone 1 exists exclusively as a lactam tautomer, either monomeric or dimeric but 3-ethoxycarbonyl-2(1*H*)-pyridone 2 exists as a lactim monomer, whereas its dimer exists in the lactam form. Despite such differences, these two compounds exhibit similar catalytic efficiencies for the reaction studied, suggesting that lactim and lactam tautomers have comparable efficiencies in tautomeric catalysis.

Introduction

Since the discovery in 1952 of the unusual catalytic efficiency of 2(1*H*)-pyridone for 2,3,4,6-tetra-*O*-methyl-α-D-glucopyranose anomeric epimerisation to the β-isomer,[1] examples of bifunctional catalytic effects have been reported for a variety of chemical reactions.[2] The attention devoted to these studies stems from the analogies between bifunctional catalyses and enzyme mediated processes.[3] All these bifunctional catalysts are tautomeric molecules or ions, usually both weak acids and weak bases. They share a common ability to bind to a reaction intermediate or transition state and to exchange simultaneously two protons while interconverting between tautomers during the catalytic process [reaction (1)]. However, whether these

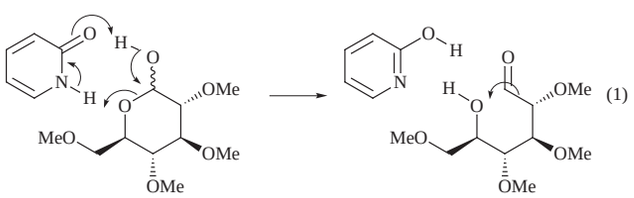

(1)

features are responsible for the catalytic efficiency is still an assumption and mechanistic studies have not yet been fully conclusive.[4]

To elucidate the role of tautomerism in these reactions, we assessed the catalytic power of lactam *vs*. lactim tautomers of 2(1*H*)-pyridone in nucleophilic aromatic substitution. To this end, substituted derivatives of 2(1*H*)-pyridone, 3-ethylaminocarbonyl-2(1*H*)-pyridone **1** and 3-ethoxycarbonyl-2(1*H*)-pyridone **2**, were prepared. As shown by NMR and UV spectroscopy, the tautomeric equilibria of **1** and **2** in $CHCl_3$ are considerably different although their structures are similar. In **1**, an intramolecular hydrogen bond involving the amide N–H stabilises the lactam form of the heterocycle, thus allowing an equilibrium between a lactam dimer and a lactam monomer. Intramolecular hydrogen bonding in **2** involves the ester carbonyl group and stabilises a lactim monomer. These two compounds could then be considered as models of lactam and lactim monomeric forms, respectively, of 2(1*H*)-pyridone. The

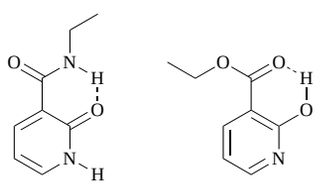

1 **2**

catalytic efficiency of **1** and **2** in the substitution of 2-fluoro-5-nitrobenzonitrile by a secondary amine was determined and correlated to their tautomeric properties.

The name '2-hydroxypyridine' will be used to designate this compound or any derivative whatever tautomeric forms, either monomeric or dimeric, may exist in solution.

Results and discussion

Synthesis

Amide **1** and ester **2** were prepared from 2-hydroxynicotinic acid *via* the corresponding acid chloride. Because they do not dimerise or tautomerise, the *N*-methyl **1a** and **2a**, and *O*-methyl derivatives **1b** and **2b** were synthesised as reference compounds for the spectroscopic studies.

Alkylation of **1** and **2** with methyl iodide in basic media yielded mixtures of *N*-methyl and *O*-methyl derivatives that could be separated by column chromatography. The regioselectivity could be directed towards either *N*-alkylation or *O*-alkylation, respectively, by the use of K_2CO_3 or Ag_2CO_3 as the basic reagent.[5] The ratios of *N*-alkylated and *O*-alkylated products as determined by ^1H NMR analysis on the crude product were as shown below.

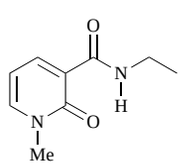

1a **1b**

	1a : **1b**
K_2CO_3	89 : 11
K_2CO_3	22 : 78

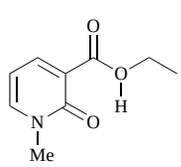

2a **2b**

	2a : **2b**
K_2CO_3	99 : 1
Ag_2CO_3	7 : 93

† Present address: Université des Sciences et Techniques de Lille (Lille 1), URA 351 du CNRS Chimie Organique et Macromoléculaire, UFR de Chimie Bâtiment C3, 59655 Villeneuve d'Ascq Cedex, France.

‡ Present address: Université Louis Pasteur (Strasbourg 1), Institut Le Bel, URA 422 du CNRS Laboratoire de Chimie Macromoléculaire, 4 rue Blaise Pascal, F-67000 Strasbourg, France.

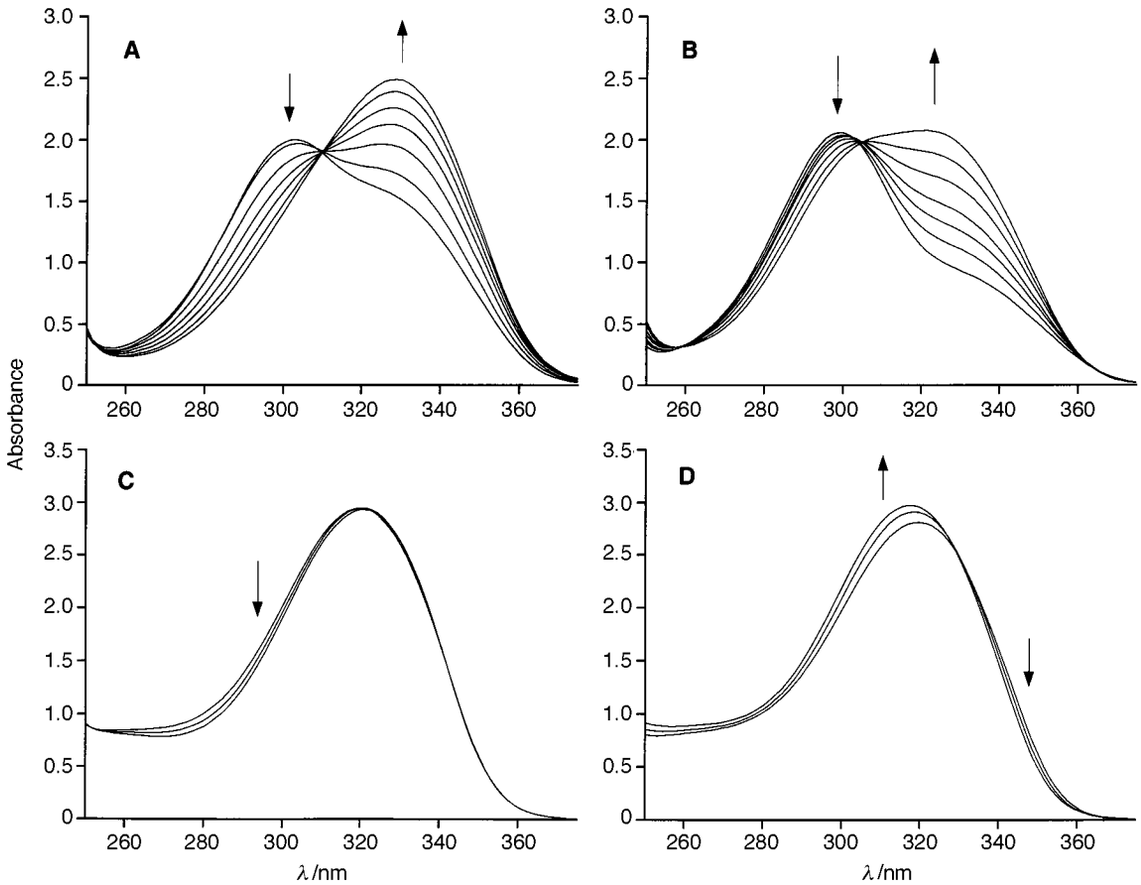

Fig. 1 UV spectra of amide **1** and ester **2** at 2 mM in $CDCl_3$. Top: spectral changes of **2** upon addition of MeOH from 0 to 1.6 M (A), and upon cooling from 57 to 4 °C (B). Bottom: spectral changes of **1** upon addition of MeOH from 0 to 1.6 M (C) and upon cooling from 53 to 12 °C (D).

Tautomerism and dimerisation

Interconversion of tautomers, solvation, and dimerisation of 2(1*H*)-pyridone result in a number of equilibria (Scheme 1).[6]

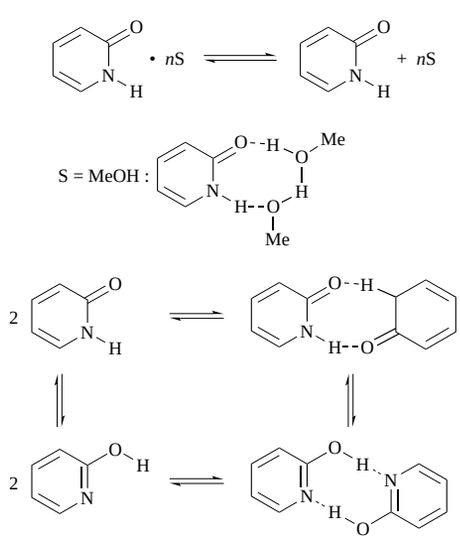

Scheme 1 Tautomerism and dimerisation of 2-pyridones. Hetero dimers between lactim and lactam tautomers are not to be excluded.

Both calculation and experiment have shown the standard enthalpies of formation of 2(1*H*)-pyridone and 2-hydroxypyridine to be similar.[7] In solution, the lactam–lactim ratio depends on the polarity of the solvent. The lactim tautomer is a better hydrogen bond donor and acceptor and predominates as a solvated monomer in polar or protic media.[8] In apolar solvents, the tautomeric equilibrium is influenced by dimerisation. Due to its polar nature, the lactam tautomer exists predominantly as a hydrogen-bonded dimer in apolar media. On the other hand, the less polar lactim tautomer is also found as a monomer in apolar solvent.[9] The proton exchange involved in the tautomerism occurs within a dimer in apolar media, or between a monomer and the solvent in protic media.[10]

The co-existence of both tautomers for ester **2** in $CHCl_3$ was demonstrated by the presence of two absorbance maxima in its UV spectrum. Each maximum is the sum of contributions from absorbances of the monomers and/or dimers of each tautomeric species.[9] Comparison with UV spectra of the *N*-methyl and *O*-methyl derivatives allowed the assignment of lactim (300 nm) and lactam (330 nm) chromophores. Upon addition of MeOH (Fig. 1A), the lactim absorbance decreases and the lactam absorbance increases through the formation of ($\mathbf{2}_{\mathbf{lactam}}$·$MeOH_n$) complexes.[11] The tautomerism is also temperature-dependent (Fig. 1B). The lactam absorbance increases upon cooling while the lactim absorbance decreases. This is consistent with a differential stabilisation of the dimeric lactam and monomeric lactim. The monomer–dimer equilibrium shifts with temperature or concentration, which results in a shift of the tautomeric equilibrium. As previously suggested for other 3-carboxy substituted 2(1*H*)-pyridones,[9] the formation of an intramolecular hydrogen bond involving the ester carbonyl group (Fig. 1) stabilizes the lactim monomer.

In contrast, the UV spectrum of amide **1** under the same conditions consists of essentially one maximum at 320 nm. Cooling, heating, or addition of MeOH induced minimal changes (Figs. 1C and 1D). These results suggest that only the lactam is present and that its UV spectrum does not change significantly upon dimerisation or complexation with MeOH. We propose that the relative stabilisation of the lactam is due to intramolecular-hydrogen bonding between the lactam carbonyl group and the amide N–H bond. This arrangement seemingly

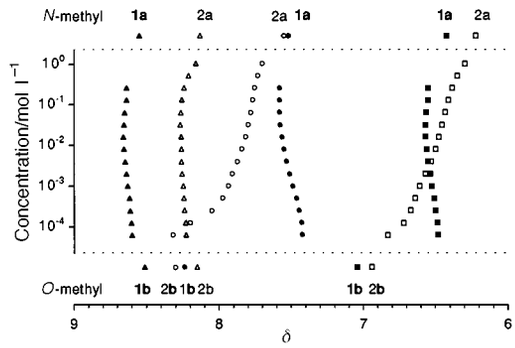

Fig. 2 ^{1}H NMR chemical shifts ($CDCl_3$, 23 °C) of H4 (▲), H5 (■) and H6 (●) signals for amide **1** and H4 (△), H5 (□) and H6 (○) for ester **2** at different concentrations. For comparison, the concentration independent shifts of the same signals for the *N*-methyl and *O*-methyl derivatives are represented above and below respectively.

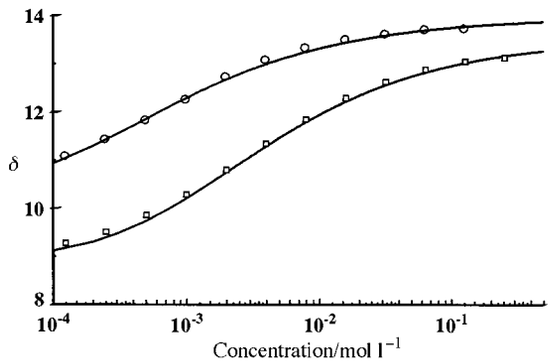

Fig. 3 Observed ^{1}H NMR ($CDCl_3$, 23 °C) chemical shift of the signals of the protomeric protons for amide **1** (□) and ester **2** (○). Data calculated for a simple dimerisation isotherm with a dimerisation constant of 280 M^{-1} for **1**, and of 1335 M^{-1} for **2** are shown as solid lines.

forms despite the possibility of a hydrogen bond between the lactim hydroxy group and the amide carbonyl.

Significant changes in the ^{1}H NMR spectra of **1** and **2** were observed upon varying concentration or temperature (shifts of up to 0.6 ppm for aromatic protons and up to 4 ppm for protomeric protons). These changes were not observed for methylated compounds **1a**, **1b**, **2a** and **2b**. As shown in Fig. 2, at a concentration of 1 mol l^{-1}, the aromatic signals of ester **2** almost match those of its *N*-methyl analogue **2a**. These signals shift toward those of the *O*-methyl derivative **2b** upon dilution. Again, these results support the hypothesis of a monomer–dimer equilibrium in which the lactam tautomer resides predominantly in dimers and the lactim tautomer in monomers [equilibria (2) and (3)]. Dilution causes dissociation of dimers and therefore a shift in the protomeric equilibrium toward the lactim tautomer.

On the other hand, at no concentration does the NMR spectrum of **1** match that of its *O*-methyl derivative. Upon dilution, H5 and H6 signals shift upfield for amide **1** whilst they shift downfield for ester **2** (Fig. 2).

These results are consistent with UV data and support the absence of the lactim tautomer for 3-ethylaminocarbonyl-2(1*H*)-pyridone **1** and a simple equilibrium between lactam monomers and lactam dimers. While the large shifts of H5 and H6 signals for the 3-ethoxycarbonyl-2(1*H*)-pyridone **2** are best explained by a lactim–lactam interconversion, the smaller shifts observed for amide **1** simply reflect the deshielding effect of the proximal carbonyl group in lactam dimers (Scheme 2). The ^{1}H NMR analysis also provides data supporting the formation of

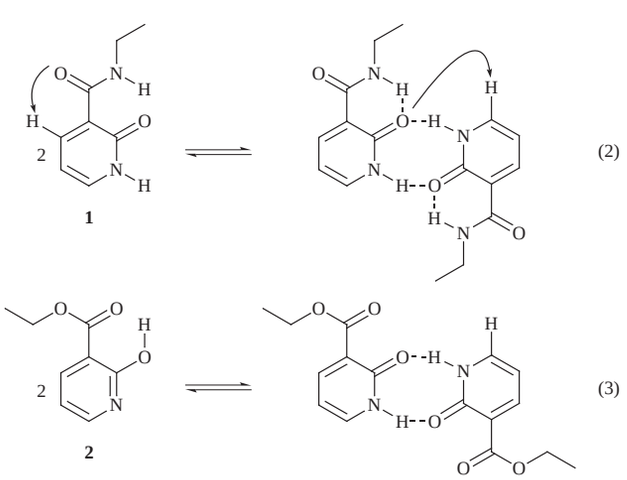

Scheme 2 Dimerisation and tautomerism of amide **1** and ester **2**. Arrows represent some of the deshielding effects observed in the ^{1}H NMR spectra.

an intramolecular hydrogen bond between the lactam carbonyl group and the amide N–H bond of amide **1**: (*i*) the chemical shift of the amide N–*H* in $CDCl_3$ is relatively far downfield (9.55 ppm) and concentration-independent; (*ii*) the deshielding effect of the carbonyl group in position 3 on the H4 signal is stronger for amide **1** (δ_{H4} 8.6) than for ester **2** (δ_{H4} 8.2) (Scheme 2).

Chemical shifts of protomeric protons of amide **1** and ester **2** are also concentration-dependent. The observed data fit a binding isotherm calculated for a simple dimerisation equilibrium,[12] which results in a sigmoidal curve when the concentration is represented on a logarithmic scale (Fig. 3).

The best fit was obtained for a dimerisation constant K_{dim} of 280 M^{-1} (estimated error margin ±10%) for amide **1**, and of 1335 M^{-1} (±15%) for ester **2**, defined as follows: 2 $[monomer]_{Total} = [dimer]_{Total}$, $K_{dim} = [dimer]_{Total}/[monomer]_{Total}^2$. The discrepancy between these values may come from repulsive secondary interactions[13] between the lactam N–H bond and the amide N–H bond in dimers of **1**. Also, the fact that the lactam oxygen of **1** partially satisfies its electrostatic demand in an intramolecular hydrogen bond might decrease its ability to form a second hydrogen bond with its remaining lone pair.

In conclusion, equilibria represented in Scheme 2 are consistent with the observed tautomeric and dimerisation properties of amide **1** and ester **2**. The next step is to evaluate how these differences affect the catalytic power of these compounds in aromatic nucleophilic substitutions.

Catalysis

The efficiency of pyridones for catalysing aromatic nucleophilic substitutions was first demonstrated by Pietra and Vitali using 2,4-dintrofluorobenzene and piperidine as reagents.[2d] As shown in Scheme 3, the proposed mechanism involves complexation of the zwitterionic intermediate by pyridone. This complex, where the oxo group and the tautomeric hydrogen of pyridone are hydrogen bonded respectively to the ammonium proton and to the electronegative fluorine atom, gets transformed into products through a cyclic transition state, by concerted departure of ammonium proton and fluoride anion from the intermediate. This process leaves the catalyst as a tautomeric hydroxy form. We studied the catalytic efficiency of amide **1**, ester **2** and 2(1*H*)-pyridone itself in the substitution of fluoride by piperidine in 2-fluoro-5-nitrobenzonitrile **3**. The cyano compound was preferred over the trifluoromethyl analogue whose reaction with piperidine is very slow.[14] Also the nitro derivative was avoided to prevent complications due to intramolecular hydrogen bonding between the nitro group and the ammonium proton in the intermediate.[15]

Since the tetrahedral intermediate may collapse to form the products or the starting reagents (Scheme 3),[16] the apparent rate constant can be expressed by eqn. (4), where k_1 and k_{-1} are the

Table 1 Apparent second order rate constants k_{app} for the piperidino-substitution of 2-fluoro-5-nitrobenzonitrile **3** in $CHCl_3$ at 25 °C in presence of 2(1*H*)-pyridone, 3-ethylaminocarbonyl-2(1*H*)-pyridone **1** or ethoxycarbonyl-2(1*H*)-pyridone **2**

[Pyridone]^a/mol l^{-1}	k_{app}/l mol^{-1} s^{-1}	[**1**]^b/mol l^{-1}	k_{app}/l mol^{-1} s^{-1}	[**2**]^b/mol l^{-1}	k_{app}/l mol^{-1} s^{-1}
5.70×10^{-5}	4.03×10^{-3}	1.01×10^{-5}	4.22×10^{-3}	1.28×10^{-5}	4.25×10^{-3}
1.14×10^{-4}	3.74×10^{-3}	1.01×10^{-4}	4.16×10^{-3}	1.28×10^{-4}	4.29×10^{-3}
5.70×10^{-4}	4.99×10^{-3}	5.05×10^{-4}	4.48×10^{-3}	5.13×10^{-4}	4.56×10^{-3}
1.14×10^{-3}	5.43×10^{-3}	1.01×10^{-3}	4.68×10^{-3}	1.03×10^{-3}	4.72×10^{-3}
5.70×10^{-3}	7.70×10^{-3}	5.05×10^{-3}	5.86×10^{-3}	2.26×10^{-3}	5.04×10^{-3}
1.14×10^{-2}	9.05×10^{-3}	1.01×10^{-2}	6.72×10^{-3}	5.13×10^{-3}	5.59×10^{-3}
4.52×10^{-2}	1.69×10^{-2}	5.05×10^{-2}	1.09×10^{-2}	1.03×10^{-2}	6.08×10^{-3}
8.33×10^{-2}	2.35×10^{-2}	1.01×10^{-1}	1.40×10^{-2}		
1.13×10^{-1}	2.64×10^{-2}				

^{a} [Piperidine] = 1.62×10^{-3} mol l^{-1}; [2-fluoro-5-nitrobenzonitrile] = 8.93×10^{-5} mol l^{-1}. ^{b} [Piperidine] = 1.64×10^{-3} mol l^{-1}; [2-fluoro-5-nitrobenzonitrile] = 9.22×10^{-5} mol l^{-1}.

Table 2 Non-linear least-square regression analysis of measured apparent second order rate constants (k_{app}) using the eqn. (6)

Catalyst	$K_{dim} \pm s_1$ [a]	$(k_1k_2/k_{-1} \pm s_2)$/ 10^{-3} l mol^{-1} s^{-1} [b]	$(k_1k_3/k_{-1} \pm s_3)$/ l^2 mol^{-2} s^{-1} [b]	(k_3/k_2)/l mol^{-1}
2(1*H*)-Pyridone	2880 ± 115	3.23 ± 0.37	5.27 ± 0.37	1631 ± 270
Amide **1**	280 ± 12	4.12 ± 0.03	0.781 ± 0.04	190 ± 10
Ester **2**	1335 ± 217	4.23 ± 0.03	1.06 ± 0.16	250 ± 30

[a] K_{dim} values were measured by NMR dilution experiments; s_1: standard deviation of K_{dim} as determined by the curve fitting program. [b] s_2: standard deviation of k_1k_2/k_{-1}; s_3: standard deviation of k_1k_3/k_{-1}; s_2 and s_3 are the sum of the standard deviation determined by the curve fitting program, and of the deviation due to the error on K_{dim}.

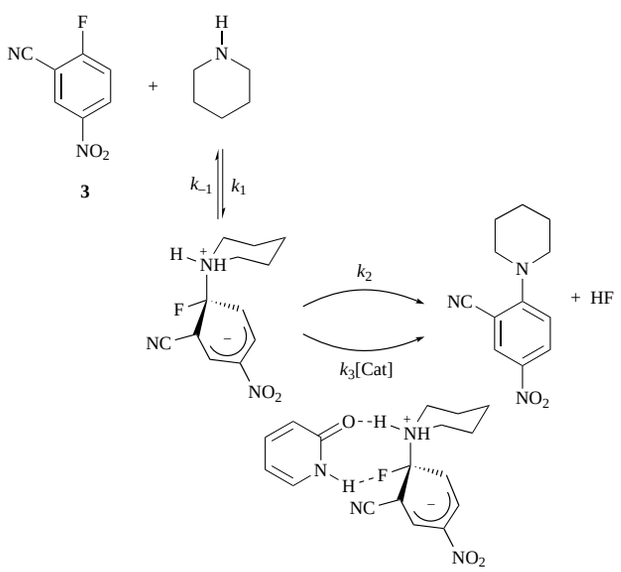

Scheme 3 Mechanism of a nucleophilic aromatic substitution. The breakdown of the intermediate into products can either take place directly (k_2) or be catalysed by the pyridone (k_3[Cat]).

$$k_{app} = k_1(k_2 + k_3[Cat])/(k_{-1} + k_2 + k_3[Cat]) \quad (4)$$

rate constants relative to the formation of the zwitterionic intermediate, respectively for forward and backward reactions, and k_2 and k_3 are the rate constants relative to the formation of products, respectively, *via* the non-catalysed and the catalysed routes.

In chloroform $k_{-1} \gg k_2 + k_3[Cat]$, the second step is then rate-limiting, and the apparent rate constant is a linear function of the concentration of catalysts [17] [eqn. (5)].

$$k_{app} = k_1k_2/k_{-1} + [Cat]k_1k_3/k_{-1} \quad (5)$$

In Table 1 are reported the measured k_{app} values at different concentrations of **1**, **2** and 2(1*H*)-pyridone. These values do increase with the total concentration of catalyst, but less than predicted by the linear relationship mentioned above (Fig. 4).

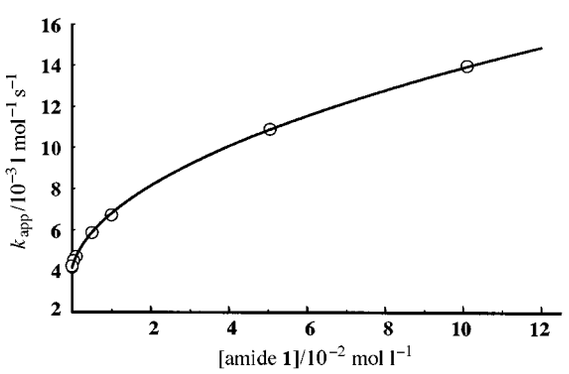

Fig. 4 Apparent second order rate constants as a function of the total concentration of 3-ethylaminocarbonyl-2(1*H*)-pyridone **1**. Data fitted according to the proposed model are displayed as a solid line.

The variations of k_{app} as a function of the concentration in monomeric catalyst can also be estimated, the concentration in monomers being expressed as a function of the total concentration in catalyst [Cat] and the dimerisation equilibrium constant K_{dim}, [Cat] = [monomeric Cat] + 2 [dimeric Cat] and K_{dim} = [dimeric Cat]/[monomeric Cat]^2 gives eqn. (6).

$$[\text{monomeric Cat}] = [(1 + 8K_{dim}[Cat])^{\frac{1}{2}} - 1]/4K_{dim} \quad (6)$$

The plot thus obtained is a straight line. Thus, the measured k_{app} values were fitted to eqn. (7) by non-linear least square

$$k_{app} = k_1k_2/k_{-1} + [\text{monomeric Cat}]\, k_1k_3/k_{-1} \quad (7)$$

regression analysis, using the K_{dim} values obtained from the analysis of the data measured by NMR spectroscopy in dilution experiments. The calculated values thus obtained for k_1k_2/k_{-1}, k_1k_3/k_{-1} and K_{dim} are reported in Table 2. The reasonable homogeneity of the values calculated for k_1k_2/k_{-1} (uncatalysed pathway) indicate that although simple, the model gives a reliable description of the reaction. The deviation observed in the variations of k_{app} with the total concentration of catalyst can thus be explained by the dimerisation of the catalyst that takes place at higher concentrations, leaving pyridones as associated

species less available for catalysis. Pyridone dimers do not participate in catalysis; only monomers are effective.

The efficiency of the catalysts tested is best expressed by k_3/k_2. It varies from 200–300-fold accelerations for **1** and **2** and to 1600-fold for 2(1*H*)-pyridone. The small difference between the catalytic efficiencies of **1** and **2** sharply contrasts with their largely different behaviours toward dimerisation and tautomerism noted from the NMR and UV studies. Ester **2** has a better hydrogen bonding ability (a larger K_{dim} value) than **1**, but this does not significantly enhance its catalytic power. Furthermore, the fact that **1** is exclusively lactam, whilst **2** is predominantly lactim, in the monomeric form does not affect the catalysis either. Each catalytic step induces interconversion of tautomers, but all the steps involved in the interconversion between tautomeric forms are faster than the aromatic nucleophilic substitution and the more stable tautomer is quickly regenerated.[10] Unless hydrogen bonding ability and tautomerism compensate for each other, it appears that these factors are not essential for catalytic efficiency.

Both 3-ethylaminocarbonyl-2(1*H*)-pyridone **1** and 3-ethoxycarbonyl-2(1*H*)-pyridone **2** are both less effective than 2(1*H*)-pyridone. A possible explanation may be that intramolecular hydrogen bonding in monomers for both amide **1** and ester **2** involves the lactam (or lactim) function. If the additional stabilisation of one tautomer by hydrogen bonding results in slower tautomer interconversion, it may also decrease the rate of proton exchange with the ammonium intermediate in the catalytic process. The proton exchange could also be dependent upon the acid–base properties of 2(1*H*)-pyridones. Regardless of which tautomer is stabilised, the electron-withdrawing substituent in position 3 for amide **1** and ester **2** tends to increase their basicity and decrease their acidity. Indeed, the measured pK_a values (10.5 and 10.7, respectively) are about one unit lower than that of 2(1*H*)-pyridone (11.62).[18]

Conclusions

In conclusion, we have developed a simple kinetic model for a reliable evaluation of the catalytic efficiency 2(1*H*)-pyridones in aromatic nucleophilic substitutions. Correlation of the catalytic potential of amide **1** and ester **2** with their physical properties enabled us to assess the role of different factors in tautomeric catalysis: dominant tautomer, hydrogen bonding ability, tautomer interconversion rate, and acid–base properties. Our results suggest that the first two properties do not account for the catalytic power of the 2(1*H*)-pyridones studied. Further work using 2(1*H*)-pyridones with various substituents is now in progress. It should provide more information and help unravel the critical criteria for large rate accelerations.

Experimental

General

^{1}H NMR measurements were performed on a Bruker AC-250 spectrometer, and a Varian VXR-500 spectrometer. NMR characterisation of **1** and **2** was performed in [$^2H_6$]DMSO as the signals are not concentration dependent in this solvent. Chemical shifts are reported in parts per million (δ) relative to the residual solvent peak. Coupling constants are given in Hertz. IR measurements were performed using a Nicolet Impact 400D instrument. Melting points were obtained on a Büchi 510 apparatus and are uncorrected. Absorbance measurements were performed on a lambda 2 Perkin-Elmer UV–VIS spectrometer controlled by the PECSS software package. Kinetic measurements were performed on a DU 7400 Beckmann UV–VIS spectrometer.

Tetrahydrofuran (THF) was distilled from sodium benzophenone–ketyl anion radical, CH_2Cl_2 was distilled from CaH_2 and hexane from P_2O_5. $CDCl_3$ was stored over molecular sieves. HPLC grade $CHCl_3$ (Aldrich Co.) was used for kinetic experiments without further purification. 2(1*H*)-Pyridone (Aldrich Co.) was sublimed before kinetic measurements. 2-Fluoro-5-nitrobenzonitrile,[19] 5-nitro-2-(1-piperidino)benzonitrile[20] and 4-nitro-1-(1-piperidino)-2-trifluoromethylbenzene[20] were prepared and purified according to reported methods.

NMR Spectroscopy

Assignment of resonances in the ^{1}H NMR spectra of compounds **1**, **1a**, **1b** and **2**, **2a**, **2b** in $CDCl_3$ were based on the following: (*i*) H5 signal is always at a higher field than H4 and H6 resonances and exhibits a characteristic coupling pattern; (*ii*) H4 has a higher coupling constant with H5 than with H6 (7.5 *vs*. 4.9 Hz for *O*-methyl derivatives **1b** and **2b**),[21] and its signal is most often at a lower field because its deshielding effect of the carbonyl in position 3 (**2b** is the only exception); (*iii*) *N*-methyl and *O*-methyl derivatives can be distinguished from the shift of the methyl group signal (4.1 ppm for O–Me and 3.6 for N–Me).

For dilution experiments, concentrated solutions of **1**, **2** or 2(1*H*)-pyridone (1 ml, in the molar range) were prepared, a 500 μl aliquot was transferred to an NMR tube and replaced by the same volume of pure solvent. The procedure was repeated down to submillimolar concentrations. Spectra were recorded with increasing acquisition times for diluted samples. Non-linear least square regression curve fitting was performed using the Axum software from MathSoft (Bagshot, UK) for determining association constants.

Kinetic measurements

The kinetics were followed spectrophotometrically at $\lambda_{anal} = 370$ nm. At this wavelength, the molar extinction coefficient of 2-fluoro-5-nitrobenzonitrile is $\varepsilon_{anal} = 15\,700$ l mol^{-1} cm^{-1}. Concentrations of substrate, amine and catalyst are reported in the tables. The kinetic runs were recorded during one hour in a thermostatted cell at 25 °C. The k_{app} values were calculated for each concentration. Least-square analyses performed with the Axum software from MathSoft company (Bagshot, UK) allowed catalytic efficiencies to be calculated.

Syntheses

3-Ethylaminocarbonyl-2(1*H*)-pyridone 1. A mixture of 2-hydroxynicotinic acid (1 g, 7.2 mmol) and $SOCl_2$ (6 ml) was heated to reflux during 15 min. Excess thionyl chloride was then removed and the residual solid was dried under vacuum. The acid chloride was dissolved in anhydrous THF (10 ml), and added dropwise to a solution of $EtNH_2$ (4 ml) in anhydrous THF (10 ml) at −78 °C. The mixture was then stirred at room temperature during 12 h. Volatiles were carefully evaporated and the residue was suspended in aqueous saturated $NaHCO_3$. The product was extracted with CH_2Cl_2 (3 × 10 ml). The organic layers were combined, washed with water, dried over $MgSO_4$ and evaporated to dryness. The product was recrystallised from acetone–pentane (970 mg, 81%), mp 158 °C; δ_H(250 MHz, $CDCl_3$) 9.56 (1H, br, s), 8.67 (1H, dd, *Ja* 7.2, *Jb* 2.2), 7.59 (1H, dd, *Ja* 6.6, *Jb* 2.2), 6.58 (1H, dd, *Ja* = *Jb* 6.9), 3.51 (2H, dq, *Ja* = *Jb* 7.3), 1.27 (3H, t, *J* 7.3); δ_C(250 MHz, [$^2H_6$]DMSO) 163.39, 162.65, 144.13, 139.54, 120.88, 106.56, 33.74, 15.26 ($C_8H_{10}N_2O_2$ requires: C, 57.48; H, 5.43; N, 8.38. Found: C, 57.21; H, 5.65; N, 8.41%); ν_{max}(KBr)/cm^{-1} 3165, 3077, 3017, 2970, 2936, 2881, 1667, 1548, 1470.

3-Ethoxycarbonyl-2(1*H*)-pyridone 2. Ethanol was carefully added to the acid chloride prepared as above and the mixture was stirred at room temperature during 12 h. Solvent was evaporated to dryness. The off-white crystalline residue was sublimed, and recrystallised from acetone–hexane to yield the ester as white needles (840 mg, 70%), mp 139 °C; δ_H(250 MHz, [$^2H_6$]DMSO) 8.02 (1H, dd, *Ja* 7.1, *Jb* 2.3), 7.64 (1H, dd, *Ja* 6.7, *Jb* 2.3), 6.25 (1H, dd, *Ja* = *Jb* 6.8), 4.18 (2H, q, *J* 7.0), 1.24 (3H, t, *J* 7.0); δ_C(250 MHz, [$^2H_6$]DMSO) 165.02, 159.55, 145.42, 141.23, 120.66, 104.65, 60.53, 14.52 ($C_8H_9NO_3$ requires: C,

57.48; H, 5.43; N, 8.38. Found: C, 57.53; H, 5.40; N, 8.34%); ν_{max}(KBr)/cm^{-1} 3197, 3087, 2971, 1721, 1665, 1596, 1556, 1480, 1430.

General methylation procedure. A mixture of the starting 2-hydroxypyridine (1 mmol) and K_2CO_3 (or Ag_2CO_3) (0.5 g) was suspended in hexane (20 ml). Methyl iodide (2 ml) was added and the mixture was stirred at room temperature during 12 h, then heated to reflux during 1 h. After cooling, CH_2Cl_2 (20 ml) was added and the mixture was stirred vigorously. Remaining solids were filtered and the filtrate was evaporated. The residue was chromatographed on silica gel, eluting with Et_2O to yield the desired compound.

3-*Ethylaminocarbonyl*-1-*methyl*-2(1H)-*pyridone* **1a**.—δ_H(250 MHz, $CDCl_3$) 9.74 (1H, br s), 8.55 (1H, dd, *Ja* 7.2, *Jb* 2.2), 7.52 (1H, dd, *Ja* 6.6, *Jb* 2.2), 6.42 (1H, dd, *Ja* = *Jb* 6.9), 3.65 (3H, s), 3.51 (2H, dq, *Ja* = *Jb* 7.3), 1.25 (3H, t, *J* 7.3).

3-*Ethylaminocarbonyl*-2-*methoxypyridine* **1b**.—δ_H(250 MHz, $CDCl_3$) 8.51 (1H, dd, *Ja* 7.5, *Jb* 2.0), 8.24 (1H, dd, *Ja* 4.9, *Jb* 2.1), 7.89 (1H, br s), 7.04 (1H, dd, *Ja* 7.5, *Jb* 4.9), 4.09 (3H, s), 3.48 (2H, dq, *Ja* = *Jb* 7.3), 1.25 (3H, t, *J* 7.3).

3-*Ethoxycarbonyl*-1-*methyl*-2(1H)-*pyridone* **2a**.—δ_H(250 MHz, $CDCl_3$) 8.13 (1H, dd, *Ja* 7.2, *Jb* 2.2), 7.55 (1H, dd, *Ja* 6.6, *Jb* 2.2), 6.22 (1H, dd, *Ja* = *Jb* 6.9), 4.36 (2H, q, *J* 7.2), 3.59 (3H, s), 1.38 (3H, t, *J* 7.2).

3-*Ethoxycarbonyl*-2-*methoxypyridine* **2b**.—δ_H(250 MHz, $CDCl_3$) 8.30 (1H, dd, *Ja* 4.9, *Jb* 2.0), 8.15 (1H, dd, *Ja* 7.5, *Jb* 2.0), 6.94 (1H, dd, *Ja* 7.5, *Jb* 4.9), 4.36 (2H, q, *J* 7.2), 4.04 (3H, s), 1.38 (3H, t, *J* 7.2).

References

1 C. G. Swain and J. F. Brown Jr., *J. Am. Chem. Soc.*, 1952, **74**, 2538.
2 (*a*) P. R. Rony, *J. Am. Chem. Soc.*, 1969, **91**, 6090 and references cited therein; (*b*) H. T. Openshaw and N. Whittaker, *J. Chem. Soc.*, *C*, 1969; (*c*) C.-W. Su and J. W. Watson, *J. Am. Chem. Soc.*, 1974, **96**, 1854; (*d*) F. Pietra and D. Vitali, *Tetrahedron Lett.*, 1966, **46**, 5701.
3 W. P. Jencks, *Catalysis in Chemistry and Enzymology*, Dover Publications, Inc., New York, 1987, 200.
4 (*a*) K.-Å. Engdahl, H. Bivehed, P. Ahlberg and W. H. Saunders Jr., *J. Am. Chem. Soc.*, 1983, **105**, 4767; (*b*) M. Kusuya, A. Noguchi and T. Okuda, *Bull. Chem. Soc. Jpn.*, 1984, **57**, 3461.
5 For a survey of alkylation methods, see: D. L. Comins and G. Jianhua, *Tetrahedron*, 1994, **35**, 2819 and references cited therein.
6 M. Gallant, M. T. P. Viet and J. D. Wuest, *J. Am. Chem. Soc.*, 1991, **113**, 721.
7 (*a*) R. S. Brown, A. Tse and J. C. Veredas, *J. Am. Chem. Soc.*, 1980, **102**, 1174; (*b*) A. Sygula, *J. Chem. Res.* (*S*), 1989, 56.
8 P. Beak, J. B. Covington and J. M. White, *J. Org. Chem.*, 1980, **45**, 1347.
9 P. Beak, J. B. Covington, S. G. Smith, J. M. White and J. M. Zeigler, *J. Org. Chem.*, 1980, **45**, 1354.
10 (*a*) M. Chevrier, J. Guillerez and J.-E. Dubois, *J. Chem. Soc.*, *Perkin Trans. 2*, 1983, 979; (*b*) O. Bensaude, M. Chevrier and J.-E. Dubois, *J. Am. Chem. Soc.*, 1978, 100, 7055.
11 T. Kitagawa, K. Matsumoto and E. Hirai, *Chem. Pharm. Bull.*, 1978, **26**, 1415.
12 C. S. Wilcox, *Frontiers in Supramolecular Organic Chemistry and Photochemistry*, ed. H.-J. Schneider and H. Dürr, VCH Weinheim, New York, 1991.
13 W. L. Jorgensen and J. Pranata, *J. Am. Chem. Soc.*, 1990, **112**, 2008.
14 R. E. Akpojivi, T. A. Emokpae and J. Hirst, *J. Chem. Soc.*, *Perkin Trans. 2*, 1994, 443.
15 C. F. Bernasconi and R. H. de Rossi, *J. Org. Chem.*, 1976, **41**, 44.
16 N. S. Nudelmann, P. M. E. Mancini, R. D. Martinez and L. R. Vottero, *J. Chem. Soc.*, *Perkin Trans. 2*, 1987, 951.
17 J. F. Bunnett and R. H. Garst, *J. Am. Chem. Soc.*, 1965, **87**, 3875.
18 A. Albert and J. N. Phillips, *J. Chem. Soc.*, 1956, 1294.
19 J. F. K. Wilshire, *Aust. J. Chem.*, 1967, **20**, 1663.
20 J. D. Hepworth and P. Jones, *Synthesis*, 1974, 874.
21 H. Günter, *NMR Spectroscopy*, Wiley, New York, 1987, 113.

Paper 7/06533G
Received 8*th September* 1997
Accepted 7*th January* 1998